MINERALOGICAL MAGAZINE, DECEMBER 1978, VOL. 42, PP. 487-92

Tin-rich garnet, pyroxene, and spinel from a slag

B. C. M. BUTLER

Department of Geology and Mineralogy, Parks Road, Oxford OX1 3PR

SUMMARY. Garnet containing up to 26% SnO_2, and pyroxene and spinel containing 12% and 10% SnO_2 respectively, occur in a tin-refining slag in association with cassiterite. These tin contents probably represent minimum values for the limit of ionic replacement of Sn^{4+} in the structure of these minerals. The absence of tin from coexisting melilite suggests that Sn^{4+} is only able to substitute for ions in octahedral co-ordination.

MANY metallurgical refining slags have a composition within the system CaO-Fe-oxide-Al_2O_3-SiO_2. Consequently they crystallize to give phases such as pyroxene, olivine, melilite, plagioclase, garnet, spinel, and other minerals that occur in natural rocks, together with phases which are less commonly found in geological environments. The petrology and mineralogy of slags is of interest to the geologist and mineralogist because of the information they can sometimes provide about natural processes and mineral compositions.

The first stage of pyrometallurgical extraction is normally one of reducing the ore to an impure metal, which contains those elements that are more easily reduced than the principal component of the ore. The second stage is to refine the impure metal by oxidation of the impurities, usually under a slag that has the metallurgical function of accommodating the oxidized impurities; in this stage a small proportion of the primary metal is usually oxidized and enters the slag. Further stages of treatment of the slag may be necessary in order to minimize metal losses in this second-stage slag.

Tin offers exceptional problems in extractive metallurgy because of the wide range of impurities in the ore and because of the similarity of behaviour of tin and iron in reducing and oxidizing conditions, and the consequent difficulty of separating pure tin. Details of the process of extracting and refining tin are given by Wright (1966).

This paper describes the mineralogy of a second-stage tin-refining slag, with a composition of which 94% lies in the system CaO-Fe-oxide-Al_2O_3-SiO_2-SnO_2. It crystallized to form garnet, pyroxene, melilite, and spinel, in association with free SnO_2 as cassiterite.

Analytical technique. All the chemical analyses were made using a Cambridge Scientific Instruments Microscan 9 electron probe microanalyser; the ZAF computer correction program of Boyd, Finger, and Chayes (1968) was used to process the data. The interference of the Sn-$L\beta_1$ line at the position of the Ca-$K\alpha$ line was determined and was found to be 2·2% of the count rate for the Sn-$L\alpha$ line this corresponded to a maximum correction of 0·15% of the Ca-$K\alpha$ count rate for garnets containing large amounts of Sn, and a negligible correction for all other phases.

The accuracy of determination of the major elements was established by analysis of a tin garnet of the composition given in Table I. This garnet was synthesized from a mixture of $CaCO_3$, Fe_2O_3, Al_2O_3, SnO_2, and SiO_2 in the proportions to give the composition $Ca_3Fe_{1.5}Al_{0.5}SnSi_2O_{12}$. Two per cent of anhydrous LiF was added to the mixture; it was heated at 880 °C for 24 hours to remove CO_2, and then at 1100 °C for 72 hours to synthesize the garnet and volatilize the LiF. The sintered mass was polished and carbon coated in the same way as the samples of tin slag. Electron probe microanalysis of each of the elements was made at twenty-four different sample positions in the conventional analysis mode of the instrument. In the case of SnO_2 the data in column II were obtained by measurement at the same twenty-four sample positions but without movement of the spectrometer between measurements. The similarity of these data to the values for SnO_2 in column I shows that the large standard deviation for this oxide and for SiO_2 is due to incomplete homogenization of the garnet during synthesis. All the data were processed using the ZAF computer correction program.

All the analyses quoted in Tables II and III represent the mean composition of at least five and usually ten points on each phase, except for the garnets in which the compositional zoning precluded repetitive analyses of different points.

Sampling. Two samples were obtained from a tin-refining slag that had been cast into a hemispherical

TABLE I. *Electron probe microanalysis of a synthetic tin-rich garnet*

	CaO	Fe_2O_3	Al_2O_3	SnO_2 I*	SnO_2 II*	SiO_2	Total
A. Composition (wt. %) as synthesized from oxides and $CaCO_3$	28·80	20·51	4·37	25·80	(25·80)	20·52	100·00
B. Composition (wt. %) as analysed (corrected for ZAF)	28·58	20·30	4·39	25·52	(25·44)	20·63	99·42
Standard deviation (24 measurements)	0·31	0·52	0·39	1·22	(1·19)	0·79	
Bias: B–A (wt. %)	−0·22	−0·21	+0·02	−0·28	(−0·36)	+0·11	

* SnO_2-I and all other oxides were determined in the conventional analysis mode; SnO_2-II was determined at the same sample positions but without movement of the spectrometer.

ladle about 1 m in diameter. The slag formed a layer about 50 cm thick above a solidified pool of partially refined metal in the base of the ladle.

A sample of fine-grained slag was obtained from the top centre of the layer, where the molten slag cooled quickly in contact with air; the second, coarser-grained and more slowly cooled, sample was from 10 to 20 cm below the upper cooling surface, with its lower surface adjacent to a large contraction cavity at the centre of the slag layer. The contraction cavity was partially filled with a friable network of cassiterite needles and spinel octahedra.

The quickly cooled slag is fine grained, and variable in colour from dark grey to mottled pale grey and black; the mottling is due to patchy distribution of areas that are completely crystalline and areas that have a very fine-grained, possibly devitrified, groundmass. The slowly cooled slag is more coarsely crystalline, and greenish black in colour. Cassiterite needles are the only recognizable phase on broken surfaces of both samples.

Chemistry of the slag. Both samples are inhomogeneous in thin section, with opaque spinel occurring as clusters and lines of crystals separated by areas containing little spinel. However, both slags are similar in bulk chemical composition, as shown by similar count rates for the major elements by X-ray fluorescence spectrometry of samples obtained by crushing large volumes of each slag; and it would appear that little fractionation occurred on cooling. The bulk chemical composition of the quickly cooled slag was determined by electron probe microanalysis of the glass prepared by fusing a sample of the powdered slag in a Pt crucible in air at 1280 °C. The analysis (corrected for ZAF) is: SiO_2 27·94, TiO_2 1·30, Al_2O_3 11·26, Fe_2O_3 (total iron) 25·16, MnO 0·30, MgO 0·98, CaO 23·25, ZnO 0·35, SnO_2 6·78, Na_2O 2·11, K_2O 0·36, total 99·79 %. X-ray fluorescence spectrometry showed the presence of trace amounts of Pb, Ta, Cr, Nb, Zr, and rare-earth elements.

Petrography. The minerals (and their approximate proportions) in the quickly cooled slag are cassiterite (2 %), opaque spinel (10 %), garnet (20 %), pyroxene (10 %), and melilite (60 %). The cassiterite occurs as colourless needles up to 1 cm long and 0·02 mm square in cross-section; all the needles have an overgrowth of garnet, up to 0·05 mm thick, zoned from deep yellow-brown and isotropic adjacent to the cassiterite to colourless and anisotropic at the edges. Single crystal X-ray diffraction photographs show no detectable epitaxial relationship between the cassiterite and the garnet. The spinel forms octahedral and sometimes skeletal crystals up to 0·5 mm across; all the spinel crystals have an overgrowth of short prisms of pyroxene, weakly pleochroic from pale green to pale yellow-brown. The melilite forms dendritic plates or prisms, up to 1 mm across, interstitial to the other minerals, but in much of the slag the interstitial material is very finely crystalline and possibly devitrified. The sequence of crystallization is primary cassiterite and spinel, followed by the overgrowths of garnet and pyroxene respectively, and finally melilite.

The slowly cooled slag, although of similar bulk chemical composition to the quickly cooled sample, has different mineralogy and microstructure. It consists of cassiterite (2 %), spinel (10 %), pyroxene (30 %), and melilite (60 %), with no garnet. The cassiterite occurs as striated orange and colourless prisms 1 cm long and up to 0·1 mm across and the spinel as octahedra and skeletal crystals up to 1 mm across. Neither mineral has the overgrowth of silicate characteristic of the quickly cooled slag. The pyroxene forms irregular prisms up to 0·5 mm long, and the melilite occurs as dendritic crystals up to 5 mm across, with a dark-coloured infilling between the branches of the dendrites, which may be glass or finely crystalline material. The sequence of crystallization is cassiterite, then spinel, then pyroxene, and finally melilite.

The occurrence of the garnet in the quickly cooled slag and the differences in microstructure between this and the slowly cooled slag require explanation. One possibility is that the garnet is stable only between the liquidus and solidus temperatures of the slag, and reacts on slow cooling to give pyroxene and melilite. Another possibility is that the garnet crystallizes metastably on rapid cooling. However, andradite garnet (without tin) is known as a mineral in steel slags, and the fact that a tin garnet of similar composition to that in the tin slag could be synthesized at 1100 °C (Table I) suggests that the former explanation is the more probable.

Chemistry of the minerals. The compositions of the minerals in the quickly cooled and slowly cooled slag samples are given in Tables II and III.

The analyses are of particular interest because the pyroxene, melilite, and spinel in the slowly cooled slag (Table III) and the garnet cores in the quickly cooled slag (Table II, col. 1*a*) occur in contact with SnO_2 as cassiterite. Their tin contents should therefore represent minimum values for the limit of ionic replacement of Sn^{4+} in the structure of these minerals (with the proviso that the garnet may be metastable, or only stable at temperatures above the solidus for the bulk composition of the slag).

The garnet core (Table II, col. 1*a*) is essentially an aluminous andradite containing one Sn ion per formula unit of 12 oxygens, giving a formula which can be written in a simplified form as $Ca_3Fe_{1\cdot5}Al_{0\cdot5}SnSi_2O_{12}$ (the composition which was selected for synthesis—see Table I). Discussion of which ion or ions replaces the depleted Si in the crystal structure will be given in the next section.

The pyroxene in the slowly cooled slag (Table III, col. 5) can be described as an aluminous hedenbergite with 0·21 Sn ions per formula unit of 6 oxygens, and the spinel (col. 7) is a magnetite with 0·16 Sn ions per formula unit of 4 oxygens.

The melilite is complex in relation to the commonly occurring end-members but can be described as containing substantial amounts of gehlenite, sodium-gehlenite, and ferro-åkermanite. It is noteworthy that tin is not detectable in this mineral.

In the quickly cooled slag the early formed spinel (Table II, col. 4) has a similar composition to that in the slowly cooled slag, but the early cassiterite is effectively screened from the later silicates by the overgrowth of garnet. Moreover, a large proportion of the SnO_2 content of the slag crystallized in

TABLE II. *Electron probe microanalyses of garnets, pyroxene, melilite, and spinel from quickly cooled slag*

	Composition (wt. %)						Atomic ratios				
	1*a* Garnet core	1*b* Garnet rim	2 Pyroxene	3 Melilite	4 Spinel		1*a* Garnet core	1*b* Garnet rim	2 Pyroxene	3 Melilite	4 Spinel
SiO_2	18·89	35·32	38·24	39·58	0·03	Si	1·83	2·88	1·56	1·89	0·00
TiO_2	3·87	1·94	1·05	0·09	1·14	Ti	0·28	0·12	0·03	0·00	0·03
Al_2O_3	4·62	9·99	12·38	10·11	3·57	Al	0·53	0·96	0·59	0·57	0·16
Fe_2O_3*	17·87	16·30	—	—	50·15	Fe^{3+}	1·31	1·00	—	—	1·47
FeO*	—	—	16·93	9·29	31·85	Fe^{2+}	—	—	0·58	0·37	1·04
MnO	0·11	0·25	0·15	0·12	0·41	Mn	0·01	0·02	0·01	0·01	0·01
MgO	0·43	1·13	3·46	1·28	1·54	Mg	0·06	0·14	0·21	0·09	0·09
CaO	27·92	31·91	23·90	31·89	0·22	Ca	2·90	2·79	1·04	1·63	0·01
ZnO	0·15	0·02	0·27	1·94	1·32	Zn	0·01	0·00	0·01	0·07	0·04
SnO_2	26·26	1·57	2·23	0·00	9·73	Sn	1·02	0·05	0·04	0·00	0·15
Na_2O	—	—	0·21	4·47	—	Na	—	—	0·02	0·41	—
K_2O	—	—	—	0·10	—	K	—	—	—	0·01	—
Total	100·12	98·43	98·82	98·87	99·96	Total cations	7·95	7·96	4·09	5·05	3·00
						Oxygens	12	12	6	7	4

* Iron oxide is assumed to be Fe_2O_3 in garnets, and FeO in pyroxene and melilite. In spinel Fe_2O_3 and FeO have been distributed to give atomic ratios in which $x = 1+y$, where x is the total of divalent ions and y is the total of quadrivalent ions.

TABLE III. *Electron probe microanalyses of pyroxene, melilite, and spinel from slowly cooled tin slag*

	Composition (wt. %)				Atomic ratios		
	5 Pyroxene	6 Melilite	7 Spinel		5 Pyroxene	6 Melilite	7 Spinel
SiO_2	32·07	40·10	0·02	Si	1·39	1·91	0·00
TiO_2	1·39	0·24	2·90	Ti	0·05	0·01	0·08
Al_2O_3	11·18	9·36	3·80	Al	0·57	0·52	0·17
Fe_2O_3*	—	—	46·26	Fe^{3+}	—	—	1·34
FeO*	16·45	10·68	34·46	Fe^{2+}	0·60	0·42	1·11
MnO	0·30	0·12	0·43	Mn	0·01	0·01	0·01
MgO	3·03	1·30	1·51	Mg	0·20	0·09	0·09
CaO	21·58	32·45	0·18	Ca	1·00	1·65	0·01
ZnO	0·26	1·00	1·00	Zn	0·01	0·04	0·03
SnO_2	12·04	0·00	10·41	Sn	0·21	0·00	0·16
Na_2O	0·52	3·78	—	Na	0·04	0·35	—
K_2O	—	0·10	—	K	—	0·01	—
Total	98·82	99·13	100·97	Total cations	4·08	5·01	3·00
				Oxygens	6	7	4

* See footnote to Table II.

the garnet cores (Table II, col. 1*a*) leaving only small amounts to enter the garnet rims and pyroxene (cols. 1*b* and 2). The simplified compositions of these two minerals are respectively an andradite–grossular and an aluminous hedenbergite, in each case with a low tin content. The melilite (col. 3) is similar to that in the slowly cooled slag, and again contains no tin.

The other element which can be regarded as exotic in relation to natural occurrences of these minerals is zinc, which is preferentially concentrated in melilite and spinel, though small amounts enter garnet and pyroxene.

The results of a step scan at 1 μm intervals from the core to the rim of a garnet crystal is given in fig. 1. The resolution, as shown by the change in count rates at the boundary between the cassiterite crystal and the garnet core, is better than 4 μm. The garnet is essentially homogeneous up to 18 μm from the core, at which point there is an abrupt change in all components except Fe_2O_3, MnO, and ZnO. The most marked changes are in the increase in SiO_2 and decrease in SnO_2, but as will be shown in the discussion this inverse behaviour of the quadrivalent oxides does not necessarily imply an ionic substitution of Sn^{4+} for Si^{4+} in the garnet structure. It is interesting to note that the other quadrivalent oxide in the composition, TiO_2, shows a slight increase at 18 μm followed by a decrease in the outer part of the rim. Calculation of atomic ratios from the weight per cent analysis shows that Ca^{2+} remains constant at 2·8 to 3·0 cations per formula unit of 12 oxygens in both core and rim. Fe^{3+} decreases from 1·3 cations in the core to 1·0 in the rim, while Al^{3+} increases from 0·5 in the core to 1·0 in the rim.

Discussion. There is little data with which to compare the garnet, pyroxene, and spinel analyses in Tables II and III. A garnet containing 14 % SnO_2 and substantial amounts of Ta_2O_5, Nb_2O_5, TiO_2, ZrO_2, WO_3, and ZnO was described by Kozlova (1969) from a tin slag. Synthetic garnets containing SnO_2 have been reviewed by Geller (1967).

The highest recorded tin content in a natural garnet appears to be 5·8 % SnO_2 in andradite in a skarn-like association of metasediments and granite pegmatites (McIver and Mihalik, 1975); lower SnO_2 contents in andradite garnet have been recorded, also from skarns (for references see McIver and Mihalik, 1975). The author has not been able to find any references to tin-bearing pyroxenes, and it is significant that in another tin-rich skarn assemblage (Mulligan and Jambor, 1968) garnet (and epidote) contain up to 2 % SnO_2, but the associated hedenbergite contains less than 70 ppm Sn. Similarly, tin does not occur in the hedenbergite of the tin-rich skarns of the Meldon area, Dartmoor, although it does occur in garnet and also forms malayaite, $CaSnSiO_5$, the tin analogue of sphene (El Sharkawi and Dearman, 1966). These data suggest that at moderate temperatures (say 500 °C) tin is unable to enter pyroxene and can

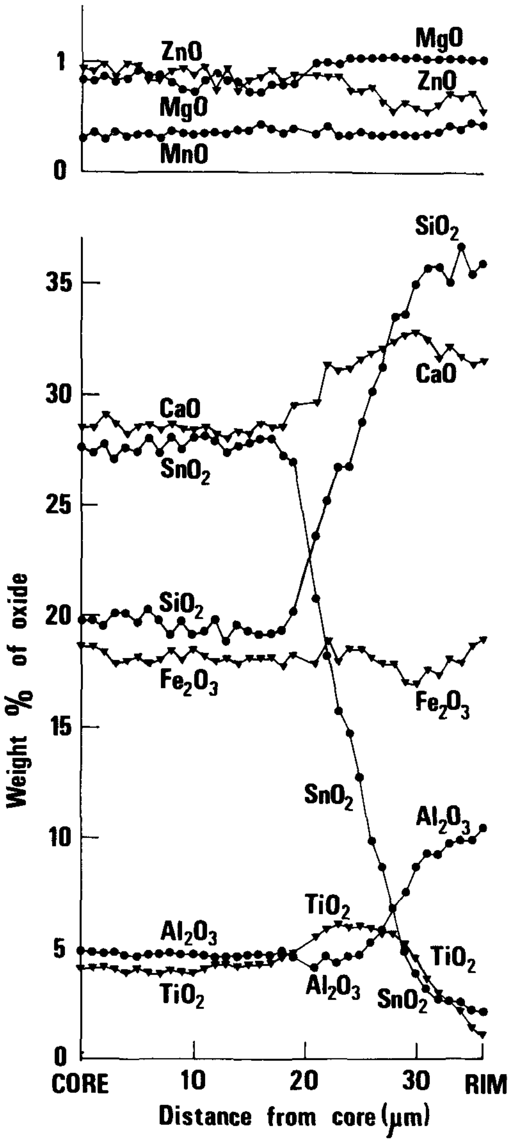

FIG. 1. Electron probe analysis of a tin-rich garnet, from core to rim.

enter garnet to a limit of about 2–5 %, while at magmatic temperatures (say 1100 °C) tin can enter both pyroxene and garnet to a limit of at least 12 % and 26 %, respectively. The possibility of using the tin contents of pyroxenes and garnets associated with cassiterite as a geological thermometer merits consideration.

The same valency and similar ionic radius of Sn^{4+} ($r = 0{\cdot}77$ Å) and Ti^{4+} ($r = 0{\cdot}69$ Å) (Whittaker and Muntus, 1970) suggest that tin could enter silicates and spinels in the same way that titanium occurs in large amounts in natural schorlomite garnet, titanaugite, and ulvöspinel from alkaline and basic igneous rocks. Geochemically tin, unlike titanium, does not crystallize in the magmatic environment that would be the natural analogue of the tin slag described here, but rather in lower-temperature mineral veins as cassiterite and in metasomatic rocks such as the skarns referred to above. The compositions of the minerals in the tin slag provide information on the crystal-chemical behaviour of tin at high temperatures, and are relevant to the frequently discussed question of ionic replacement of large quadrivalent cations such as Ti^{4+}, Zr^{4+}, and Sn^{4+} in the garnet structure (see McIver and Mihalik, 1975; Huggins *et al.*, 1977; Geller, 1967).

The contribution that the present paper is able to make to the discussion concerns the relative tin contents of garnet, pyroxene, spinel, and melilite. The structural formulae of these minerals can be written in terms of X (8-co-ordinated, large cation), Y (octahedral, intermediate-size cation), Z (tetrahedral, small cation), and O (oxygen): garnet $X_3Y_2Z_3O_{12}$; pyroxene XYZ_2O_6; spinel Y_2ZO_4; melilite $X_2Z_3O_7$. Although comparison of the site preferences of ions in structures as different as these four minerals is of dubious validity, the absence of tin from melilite, especially when compared with the large amounts in garnet, pyroxene, and spinel, suggests that tin is only able to enter Y (octahedral) sites, which are not present in melilite. From this argument the ionic replacements that allow tin to enter the other three structures would be:

Garnet	X	Y	Z	
	Ca_3^{2+}	R_2^{3+}	Si_3^{4+}	→
	X	Y	Z	
	Ca_3^{2+}	$R^{3+}Sn^{4+}$	$R^{3+}Si_2^{4+}$	
Pyroxene	X	Y	Z	
	Ca^{2+}	$Fe^{2+}Al^{3+}$	$Al^{3+}Si^{4+}$	→
	X	Y	Z	
	Ca^{2+}	$Fe^{2+}Sn^{4+}$	Al_2^{3+}	
Spinel	X	Y	Z	
	—	Fe^{2+}	Fe_2^{3+}	→
	X	Y	Z	
	—	Sn^{4+}	Fe_2^{2+}	

These conclusions are in agreement with those of Huggins *et al.* (1977) from Mössbauer spectrometry that Ti^{4+} has a low preference for the tetrahedral site compared with Al^{3+} and Fe^{3+}, and their prediction on crystal-chemical grounds that Sn^{4+} would have a still lower preference than Ti^{4+}. Further support for the proposal that Sn^{4+} can only enter the tetrahedral site with difficulty is indicated by the failure to synthesize a single-phase garnet of composition $Ca_3Fe_2Sn_3O_{12}$ (Geller, 1967). On this basis the inverse correlation of SiO_2 and SnO_2 in the zoned garnet whose composition is shown in fig. 1 is the result of charge balancing by quadrivalent ions, but the actual replacement is (Fe^{3+}, Al^{3+}) for Si^{4+} in the tetrahedral site and Sn^{4+} for (Fe^{3+}, Al^{3+}) in the octahedral site. The garnet in the tin slag is thus of different type from that described by McIver and Mihalik (1975) in which an inverse correlation of Sn and total Fe suggested a substitution $2Fe^{3+} \rightarrow (Fe^{2+}, Sn^{4+})$.

Experimental work by Huckenholz (1969) on the system $3CaO.Fe_2O_3.3SiO_2$ (andradite)-$3CaO.Fe_2O_3.3TiO_2$ ('Ti-garnet') showed a limit of garnet stability at $3CaO.Fe_2O_3.1{\cdot}5TiO_2.1{\cdot}5SiO_2$. This stoichiometric limit of composition suggests the possibility that ionic substitution of Si^{4+} by a larger cation produces an ordered structure in which only half the tetrahedral sites are available for substitution. Huckenholz also showed that ionic replacement in the system $CaMgSi_2O_6$ $CaTiFe_2O_6$ is limited to less than 5 wt.% Ti-pyroxene; this result is compatible with the lower SnO_2 content of the pyroxene compared with the garnet in the tin slag. Further work on site preferences of Sn^{4+} and Ti^{4+} in both garnets and pyroxenes would be of interest.

The oxidation state of tin oxide at high temperatures has been a problem for many years because of the similar free energies of formation of SnO and SnO_2. The determination by Carbó Nóver and Richardson (1972) indicates that above 1100 °C SnO is more stable than SnO_2 in the pure oxide system. The temperature of crystallization of the slag described here is almost certainly above 1100 °C, but the petrography of the slag suggests that SnO_2 as cassiterite crystallized as a primary phase from a completely molten liquid. The presence of cassiterite needles in the contraction cavity at the centre of the slag layer indicates that tin was still present in the quadrivalent state at the end of the crystallization history of the slag. The bulk chemical composition of the slag indicates that the solubility of SnO_2 in liquid of the composition of this slag is at least 6·8% (Table II), a value higher than that found by Shelley and Shelley (1973). Evidently more work should be done on the oxidation state and solubility of tin oxide in silicate melts.

Acknowledgements. The samples were provided by Williams, Harvey & Co. Limited, and the author gratefully acknowledges their permission to publish this paper. He is indebted to Dr. R. C. O. Gill for help with the electron probe microanalysis.

REFERENCES

Boyd (F. R.), Finger (L. F.), and Chayes (F.), 1968. *Carnegie Inst. Washington Yearbook*, **67**, 210–15.

Carbó Nóver (J.) and Richardson (F. D.), 1972. *Trans. Inst. Min. Metall.* **81**, C63–C68.

El Sharkawi (M. A. H.) and Dearman (W. R.), 1966. *Econ. Geol.* **61**, 362–9.

Geller (S.), 1967. *Z. Kristallogr.* **125**, 1–47.

Huckenholz (H. G.), 1969. *Am. J. Sci.* **267-A**, 209–32.

Huggins (F. E.), Virgo (D.), and Huckenholz (H. G.), 1977. *Am. Mineral.* **62**, 475–90.

Kozlova (B. A.), 1969. *Tr. Proekt. Nauch-Issled. Inst. 'Gipronikel'*, **42**, 78–89, [*Chem. Abstr.* **75**, 96131s].

McIver (J. R.) and Mihalik (P.), 1975. *Can. Mineral.* **13**, 217–21.

Mulligan (R.) and Jambor (J. L.), 1968. Ibid. **9**, 358–70.

Shelley (T. R.) and Shelley (R.), 1973. *Trans. Inst. Min. Metall.* **82**, C54–C56.

Whittaker (E. J. W.) and Muntus (R.), 1970. *Geochim. Cosmochim. Acta*, **34**, 945–56.

Wright (P. A.), 1966. *Extractive Metallurgy of Tin.* Elsevier, Amsterdam.

[*Manuscript received 12 January 1978*]

Note added in proof.

Mössbauer spectrometry by Dr. M. F. Thomas and Mr. J. Baines, at the Oliver Lodge Laboratory, University of Liverpool, of a garnet of composition $Ca_3Fe_2^{3+}SnSi_2O_{12}$, synthesized by the same techniques as the garnet with the composition quoted in Table I, shows that the distribution of Fe^{3+} between tetrahedral and octahedral sites is approximately 1:1. This confirms that the structural formula of the tin garnet is of the form $Ca_3(Fe^{3+}Sn)(Si_2Fe^{3+})O_{12}$.